Journal of Integrative Agriculture 2026, 25(8): 3440–3452

Available online at ScienceDirect

Journal of Integrative Agriculture



RESEARCH ARTICLE

Modelling spatio-temporal dynamics of soil organic carbon in paddy soil by coupling digital soil mapping with a process model

Zheng Wang[1, 2], Songchao Chen[1, 2, 3], Ruiying Zhao[4], Jie Xue[5], Qiangyi Yu[6], Danqing Wei[1, 2, 7], Wei Chen[8], Qichun Zhang[1, 2], Zhou Shi[1, 2#]

[1] *State Key Laboratory of Soil Pollution Control and Safety, Zhejiang University, Hangzhou 310058, China*
[2] *College of Environmental and Resource Sciences, Zhejiang University, Hangzhou 310058, China*
[3] *ZJU-Hangzhou Global Scientific and Technological Innovation Center, Zhejiang University, Hangzhou 311215, China*
[4] *Department of Geography, National University of Singapore, Singapore 117570, Singapore*
[5] *Department of Land Management, Zhejiang University, Hangzhou 310058, China*
[6] *Institute of Agricultural Resources and Regional Planning, Chinese Academy of Agricultural Sciences, Beijing 100081, China*
[7] *Zhejiang Economic Information Center, Hangzhou 310006, China*
[8] *Bureau of Agriculture and Rural Affairs of Jiashan County, Jiaxing 314100, China*

Highlights

- The Well-facilitated Farmland Construction Project can prevent soil organic carbon (SOC) loss.
- The temporal variation of SOC density (SOCD) is influenced by straw incorporation and irrigation.
- Coupling the digital soil mapping (DSM) and CENTURY is an effective approach to simulate the SOC dynamics.

Abstract

Soil organic carbon (SOC) plays a crucial role as a nutrient trigger and directly impacts soil health and agricultural productivity. In China, the Well-facilitated Farmland Construction (WFC) Project is a comprehensive agricultural management strategy, changing the soil environment and then influencing the SOC dynamics. However, the long-term trajectory of SOC under the implementation of the WFC Project remains unclear. To address this knowledge gap, this study focused on farmland in southeastern China that completed the WFC Project in 2022. A total of 202 topsoil samples (0–20 cm) were collected from the regional paddy soil in 2023. Using digital soil mapping (DSM) and the CENTURY model, we delineated key soil properties and simulated the spatio-temporal changes of SOC density (SOCD). The results revealed that the SOCD ranged from 1.23 to 6.35 kg m^{-2}, with an average value of 3.68 kg m^{-2} in 2023. Soil pH, clay, and sand content were primary factors influencing SOCD distribution. According to CENTURY model simulations, SOCD exhibited a declining trend from 2010 to 2021, while it was projected to increase from 2022 to 2030 following the WFC implementation, which could be attributed to enhancements in irrigation and straw incorporation. Besides, the scenario without WFC results shows that SOCD would decline from 2022 to 2030, underscoring the project's effectiveness in preventing SOC loss for paddy soil. The spatial patterns of SOCD in 2021 and 2030 were similar, and the low-value areas showed faster increase rates than the areas with high SOCD levels, indicating that the specific field plots with lower SOCD levels could sequester more carbon with improved soil management. In conclusion, the WFC Project can potentially increase SOC sequestration in the paddy soil and grain yield, ensuring food security and addressing climate change.

Keywords: soil organic carbon, Well-facilitated Farmland Construction, spatio-temporal variation, digital soil mapping, CENTURY model

1. Introduction

Soil is the largest carbon pool in terrestrial ecosystems and contains three times more carbon than that in the atmosphere and four times more than that in the vegetation (Lal 2013). Among the soil carbon components, soil organic carbon (SOC) in farmland is particularly crucial as it enhances soil

Received 4 July 2025; Received in revised form 24 September 2025; Accepted 9 October 2025; Available online 7 November 2025
Zheng Wang, E-mail: wangzheng96@zju.edu.cn; #Correspondence Zhou Shi, E-mail: shizhou@zju.edu.cn

© 2026 CAAS. Publishing services by Elsevier B.V. on behalf of KeAi Communications Co. Ltd. This is an open access article under the CC BY-NC-ND license (http://creativecommons.org/licenses/by-nc-nd/4.0/). Peer review under responsibility of Editorial Board of *Journal of Integrative Agriculture*.
doi: 10.1016/j.jia.2025.11.006

fertility and structure (Allison 1973; Eswaran *et al.* 1993; Franzluebbers 2002; Stockmann *et al.* 2015). Moreover, most SOC is stored in the topsoil (0–20 cm), which is also the primary nutrient source of crop growth. As a result, SOC in topsoil is often considered as a key indicator of soil quality and productivity (Allison 1973; Bauer and Black 1994; Reijneveld *et al.* 2009). However, SOC in the farmland topsoil is highly influenced by the soil intrinsic properties (e.g., soil texture and pH) and human activities (e.g., agricultural management and farmland construction), leading to significant spatio-temporal variation within farmland ecosystems (Wu *et al.* 2003; Smith 2005; Li *et al.* 2013; Sun *et al.* 2019; Long *et al.* 2020). Wherein the influence of human activities plays an important role in the farmland SOC; for example, conservation tillage with straw incorporation means that the soil is covered between the harvest and the next crop, and it can resist the influence of wind and water erosion on SOC and increases the carbon input (Seitz *et al.* 2018; Chen S *et al.* 2023; Yang *et al.* 2024). Additionally, if the farmlands are fully developed, improvements in the irrigation infrastructure, soil moisture, and crop growth can enhance plant residue production and increase carbon input to the soil (Collins *et al.* 1992). In other words, when the farmland is carried out with minimum tillage or inadequate irrigation, soil health and crop growth are affected negatively. Therefore, exploring the topsoil SOC variation in farmland is significant for soil management, agricultural sustainability, and food security (Sanderman *et al.* 2017; Chen *et al.* 2018).

Traditional soil monitoring is conducted through field investigation, and then the soil map is delineated based on expert experience. However, this approach is inefficient and inaccurate for monitoring soil dynamics (Inman *et al.* 2002). With the advances in remote sensing and computing technology, digital soil mapping (DSM) has gained widespread as a recognition framework to map the spatial distribution of different soil properties (McBratney *et al.* 2003; Lagacherie and McBratney 2006; Chen *et al.* 2022). Generally, the spatial pattern of soil properties exhibits high heterogeneity due to the influence of natural factors and human activities (Cambule *et al.* 2013; Malone *et al.* 2014). Machine learning (ML) has achieved considerable accuracy by integrating the covariates and dealing with the non-linear relationship between soil properties and environmental factors (Behrens *et al.* 2014; Minasny and McBratney 2016). Among the ML models, Random forest (RF) is an ensemble model by combining many decision trees that is widely used in DSM studies (Breiman 2001; Grimm *et al.* 2008; Dharumarajan and Hegde 2020). RF offers several advantages, including the ability to model non-linear relationships, resistance to overfitting, and a minimal need of parameter tuning (Breiman 2001; Liaw and Wiener 2002). Studies by Hengl *et al.* (2015) in Africa, Heung *et al.* (2014) in Canada, and Liu *et al.* (2022) in China have demonstrated that RF can accurately predict the spatial distribution of various soil properties.

In the past decades, the spatio-temporal dynamics of SOC have predominantly been monitored through multi-period soil sampling, but this approach is widely recognized as costly (Goidts *et al.* 2009). Although the DSM technology can provide an effective tool for the SOC spatio-temporal monitor by generating historical maps, empirical and statistical models also depend on the historical data, while obtaining a continuous time series SOC map becomes challenging when soil sampling data are unavailable for a specific year (Somaratne *et al.* 2005; Kumar *et al.* 2018; Zhang *et al.* 2024). Therefore, these constraints probably lead to the inability to explore the history and future of SOC changes without the historical and future data. Moreover, data-driven models overlook ecosystem dynamics and biogeochemical processes, making it difficult to explain the results (Zhao *et al.* 2023). At present, process-based biogeochemistry models provide a robust approach for estimating the SOC cycle. For instance, the CENTURY model is one of the most frequently used methods driven by soil and climate data to simulate the soil carbon dynamics in different ecosystems (Kelly *et al.* 1997; Tornquist *et al.* 2009; Zhang *et al.* 2020). This model demonstrates many advantages in simulating SOC dynamics across different scales, as it incorporates critical factors such as crop growth, fertilization, tillage, and irrigation through its submodels (Parton *et al.* 1988; Ouyang *et al.* 2014; Dimassi *et al.* 2018; Berardi *et al.* 2020). Furthermore, the CENTURY model can simulate monthly and annual SOC dynamics, providing valuable insights into SOC variation while reducing the costs associated with long-term soil surveys (Ogle *et al.* 2010).

Managing SOC through optimized farmland practices is one approach to enhance the soil ecosystem services and improve productivity (Blanco-Canqui *et al.* 2013; Chen *et al.* 2017). Farmland construction is one of the important management strategies by human activities, which can change the fertilization, irrigation, cultivation system, and others according to the standards set by managers, thereby affecting the SOC storage and spatio-temporal variation (Wang *et al.* 2020). In 2013, the Chinese government implemented the Well-facilitated Farmland Construction (WFC) Project and reported that all farmland in China will be constructed to be well-facilitated farmland by 2030. This nationwide project established comprehensive indicators to ensure soil health, including irrigation (adequate for crop growth), harvest (straw incorporation), the thickness of the effective soil layer (the depth over 20 cm), agricultural system (regulated crops for planting), and other indicators (NDRC 2021). These indicators can change and influence the soil texture (the component of sand, silt, and clay), moisture, evapotranspiration, and microorganisms, which are associated with the carbon cycle and sequestration. However, it is unclear whether the WFC Project will increase or decrease the SOC. Additionally, if the well-facilitated farmland is not fully developed (maintaining traditional management practices), how will SOC change in the future?

To address these hypotheses, we selected a constructed, well-facilitated farmland as the study area, using the DSM technology to predict spatial patterns of key soil properties. We further simulate SOC spatio-temporal variation by driving a process-based ecosystem model (CENTURY model) using those key soil properties of SOC. The objectives of this study are: (1) to determine the environmental factors that influence the SOC; (2) to evaluate the change of SOC before and after WFC (2010–2030); (3) to explore the spatio-temporal

distribution of the SOC in the future with built or not well-facilitated farmland. The basic workflow is shown in Fig. 1.

2. Materials and methods

2.1. Study area

The natural environment of study area The study area (30°56′–31°00′N, 120°53′–120°57′E) is located in Jiashan County, Zhejiang Province of southeastern China, with an area of approximately 9.0 km^2 (Fig. 2). The Jiashan is predominantly an alluvial plain (Hangzhou-Jiaxing-Huzhou Plain) with an average altitude of 3.6 m. The farmland is fragmented due to dense river networks, and the water area is distributed in the central part of the study area. The study area is influenced by a subtropical monsoon climate with an annual rainfall of 1,200 mm and an annual mean temperature of 15.6°C, exhibiting hot and rainy in summer while the cold and dry in winter. The study area is mainly focused on rice–wheat production in China, with agricultural activities dating back to the Hemudu Culture period. Rice is typically planted in June and harvested in November, while wheat is sown in November and harvested in May of the following year. Paddy soil is one of the anthrosols and is the primary soil type in the study area. Generally, the horizon of paddy soil is divided into submergenic, plough pan, percogenic, and parent material horizons. The soil shows weak acidity because of the humid and hot climate influence in this study area.

The differences between well-facilitated farmland and traditional farmland The study area completed the WFC Project in 2022. In comparison to traditional farmland, the WFC Project introduces two primary differences: (1) The well-facilitated farmland conducted the straw incorporation, aiming to improve the soil quality, while the aboveground crops in traditional farmland were almost harvested; (2) irrigation canals were constructed across the well-facilitated farmland to ensure water supply for crop growth. Besides, the WFC includes requirements for rice–wheat rotation, soil thickness greater than 20 cm, and soil analysis with formulated fertilization, while these strategies have been in place in previous years and continue during the implementation of the WFC Project.

2.2. Data collection

Soil sampling In this study, we used the uniform equidistant distribution to conduct the soil sampling. Firstly, the study area was separated into a 250 m×250 m grid, and the sampling sites were predesigned at the node of each grid in the laboratory (Dai *et al.* 2024; Zhou *et al.* 2025). During field sampling, we followed the predesigned site position to collect the soil materials and record the geographic coordinates of all actual sampling sites using a handheld global positioning system (GPS) device (10 m precision). Three random topsoil

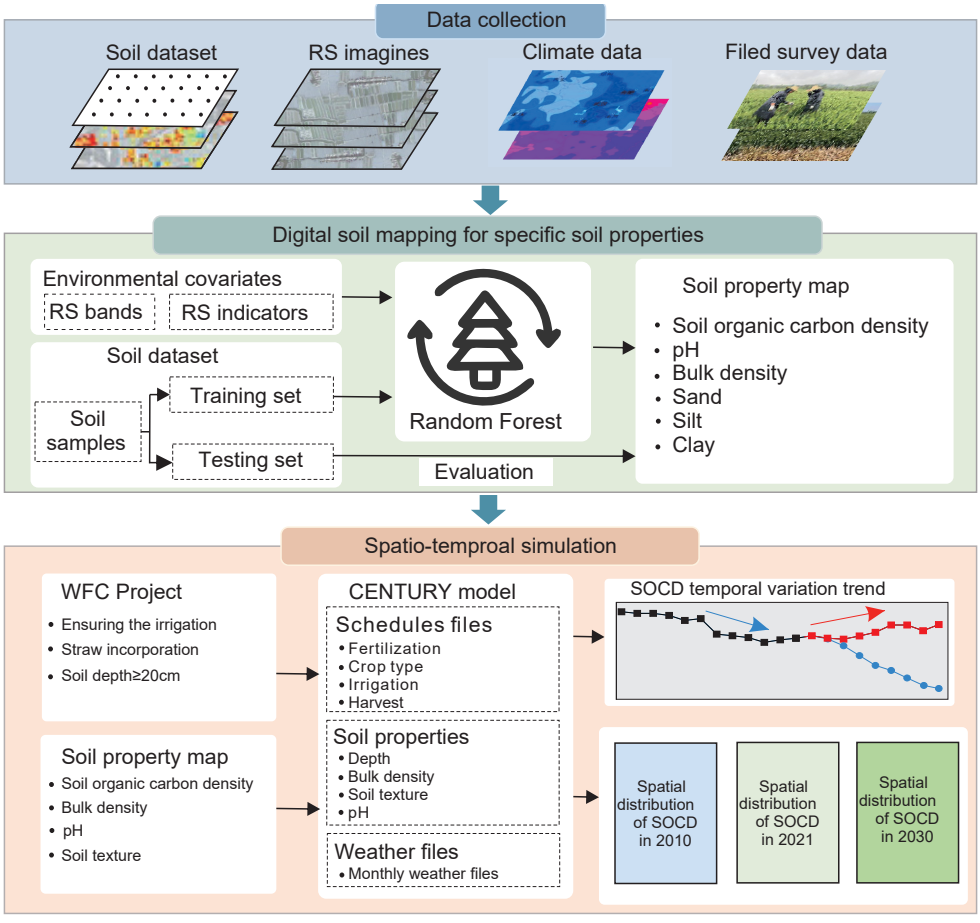
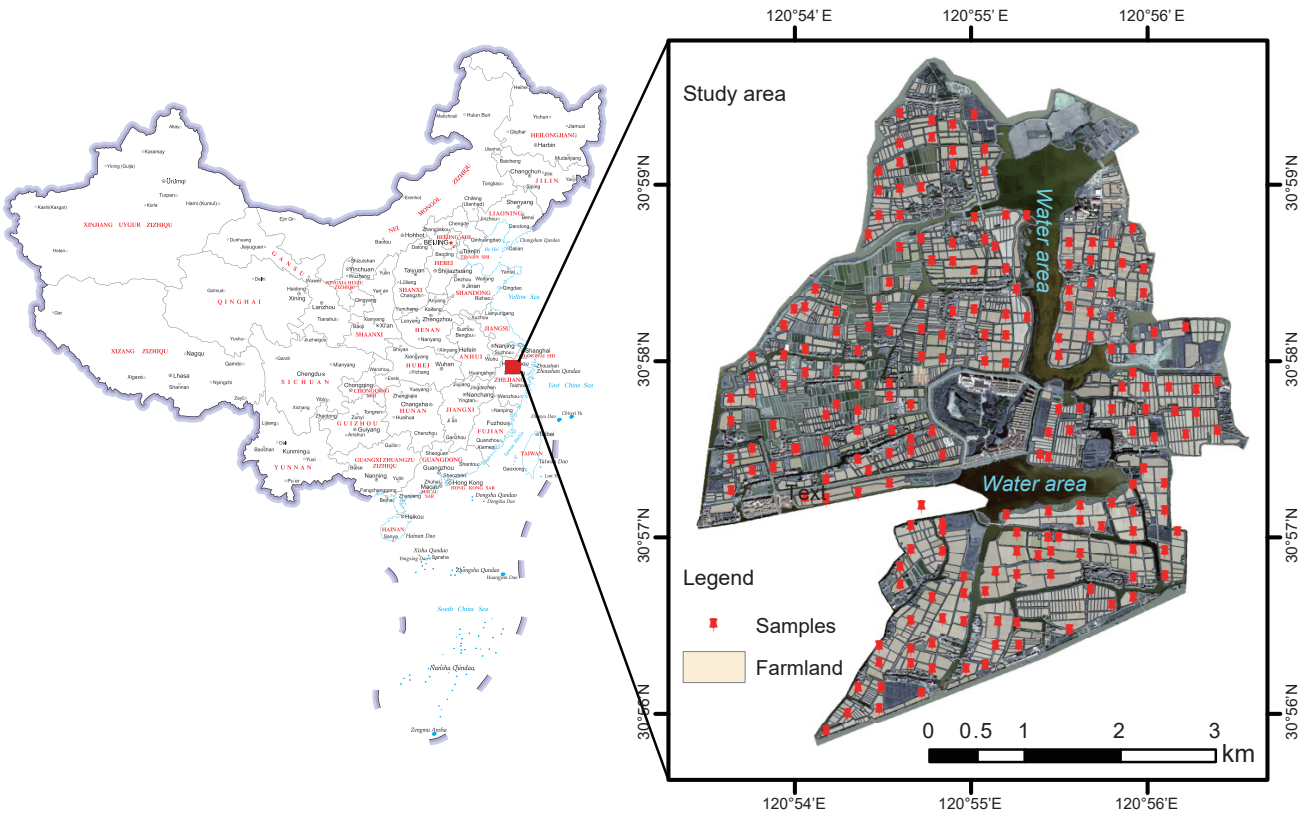


Fig. 1 The workflow of this study. RS, remote sensing; WFC, Well-facilitated Farmland Construction; SOCD, soil organic carbon density.



审图号：GS 京 (2026) 0965 号

Fig. 2 Study area and the locations of sampling sites.

subsamples (0–20 cm depth) in each site were collected, thoroughly mixed, and then sealed in plastic bags. Each sample weighed approximately 1 kg. Finally, a total of 202 soil samples were collected in May 2023 from fallow fields, after the wheat harvest and before the next planting season (Fig. 2). Before analyzing soil samples, soil materials were air-dried at around 25°C and then passed through the 2 mm sieves to remove stones and plant residues. Afterward, we measured the SOC, pH, and soil texture (clay, silt, sand) in the laboratory by standard methods (Bao 2000). Meanwhile, bulk density (BD) was measured by the cylinder with a volume of 100 cm^3 during the field sampling. The BD was calculated by the following equation:

$$BD\ (g\ cm^{-3}) = \frac{\text{The soil weight after dried (g)}}{\text{The volume of cylinder (cm}^3\text{)}} \quad (1)$$

In this study, since the CENTURY model requires SOC density (SOCD, kg m^{-2}) for model simulation, the SOCD was calculated as follows (Chen Z *et al.* 2023):

$$SOCD = SOC \times BD \times H \times \frac{1-G}{100} \quad (2)$$

where SOC, BD, H, and G were the topsoil layer SOC content (g kg^{-1}), bulk density (g cm^{-3}), soil thickness (20 cm deep in this study), and gravel contents (%), respectively. *G* is set to 0 in farmland since all of them have been removed during the long-term tillage in the study area.

Sentinel-2 data Remote sensing bands can be utilized to estimate several soil properties of surface soils because different soil properties exhibit unique absorption and reflection characteristics at specific spectral bands (Swain *et al.* 2021; Wang *et al.* 2024). Sentinel-2 loads the multi-spectral imager with 13 bands covering the visible (red, green, and blue), near-infrared (NIR), and shortwave infrared (SWIR) (Gao *et al.* 1993). Referring to the previous research (Vaudour *et al.* 2019), we collected Sentinel-2 images that corresponded to the soil sampling (May 2023) and included Band 2, Band 3, Band 4, Band 7, Band 8, Band 11, and Band 12 in the DSM framework and in this study (Appendix A).

In addition, we also used several remote-sensing indicators that are associated with soil properties to improve prediction accuracy (Ben-Dor *et al.* 2002; Liu *et al.* 2015; Jin *et al.* 2016; Gholizadeh *et al.* 2018), including the normalized differences vegetation index (NDVI), transformed vegetation index (TVI), enhanced vegetation index (EVI), soil adjusted vegetation index (SAVI), moisture stress index (MSI), green normalized difference vegetation index (GNDVI), green-red vegetation index (GRVI), land surface water index (LSWI), and vegetation index (VI). The calculation equations are shown in Appendix B.

2.3. Digital soil mapping

DSM is an effective approach to estimating the spatial distribution of various soil properties by developing regression models that relate these properties to different covariates through machine learning algorithms (McBratney *et al.* 2003; Chen *et al.* 2022; Xue *et al.* 2024). In regression cases, RF is a widely used machine learning algorithm. It built many

decision trees and averaged the predictions from each tree to calculate the final results. In this study, we used RF to conduct the DSM progress of each key soil property. To improve prediction performance, we tuned two key parameters, including *ntree* (the number of trees in the forest) and *mtry* (the number of variables considered for splitting at each tree node). Specifically, the parameters *ntree* and *mtry* were optimized within a range of 500 to 1,000 for *ntree* and from 10 to 15 for *mtry* by 5-fold cross-validation. The seven remote sensing bands and the nine critical indicators based on the Sentinel-2 image calculation mentioned in Section 2.2 were applied as environmental covariates in digital soil mapping. The RF algorithm was implemented in R 4.2.1 utilizing the *randomForest* packages (Liaw and Wiener 2002; R Core Team 2022).

2.4. CENTURY model simulation

Brief description of the CENTURY model The CENTURY model was initially developed by Parton *et al.* (1988) and designed to simulate the grassland carbon dynamics; with the model development, the CENTURY 4.7 version can be utilized in the forest and farmland ecosystem, and it has been updated with the terrestrial carbon cycle features of recent years. This version integrates key environmental factors such as temperature, soil moisture, C:N ratio, and pH (Parton *et al.* 1988).

The CENTURY model provides the default parameters initially calibrated based on ecosystems in the United States for driving simulation programs. Consequently, the parameter input should be reset according to the new environment to make the model suit the ecosystem of the study area. In this study, soil properties (pH, BD, sand, silt, and clay) predicted by DSM technology were utilized as site-specific data input for the CENTURY model to simulate the SOCD dynamic simulation of the study area; the climate data from 2000 to 2022 was collected from the Resource and Environment Science and Data Center (https://www.resdc.cn/) and used to drive the CENTURY model, standard deviations and skewness for each month, the monthly precipitation and maximum and minimum temperature was input to drive the model simulation. Detailed data inputs for the CENTURY model are presented in Appendix C.

Prior to running the historical and future simulation for each site, a long-term spin-up procedure was essential for the model simulation to ensure the soil carbon variation reaches the equilibrium state. Before the land was converted to farmland, the landscape was usually grassland (Wang *et al.* 2019). Therefore, the spin-up was executed 3,000 years with the grassland ecosystem in this study. The model was driven by precipitation and temperature of generated data based on the observed climate records from 2000 to 2022. Following the spin-up, the CENTURY model set the crop management mode to simulate the SOCD dynamic. Monthly climate data from 2000 to 2022 were collected and used to drive the model. For details about CENTURY 4.7, please refer to the model user manual (Parton *et al.* 1988).

The key parameters for simulating SOCD changes under different scenarios The primary distinctions between traditional farmland and well-facilitated farmland were irrigation and harvest. These differences were incorporated into the CENTURY model to simulate the spatio-temporal variations of SOCD; the key parameters were defined for each scenario within the model, and the details are shown in Table 1. For well-facilitated farmland, the implementation of the WFC Project ensured optimal soil layer thickness, irrigation approach, and straw incorporation, so we hypothesized that the 45% of aboveground lives would not be affected by harvest, meaning that the litter would decompose into soils, besides when available water holding capacity below 25% for wheat and 95% for rice, the irrigation would carry out; the effective soil thickness was set 0–20 cm depth. Therefore, the harvest parameter was set to 0.45; the irrigation parameters for wheat and rice in the CENTURY model were set to 0.25 and 0.95, respectively; the soil layer was set to 1, indicating a soil depth of 0–20 cm. In contrast, the harvest parameters for traditional farmland were set to 0.10, indicating that only aboveground lives of 10% were left and others were harvested; the irrigation parameters for wheat and rice were 0.15 and 0.50, representing that the farmland would be irrigated when the available water holding capacity below 10% for wheat and 50% for rice. The parameter of NLYER indicates the soil thickness and was set as 1, representing that the soil thickness was between 0 and 20 cm; the main fertilizer is the nitrogen (N) fertilizer, and the amount of N to be added for wheat and rice was 3.50 and 15.00 g N m^{-2}. These parameters referred to previous research and field investigations (Mao 2002; Yang *et al.* 2007; Dong *et al.* 2018; Wang *et al.* 2021; Liang *et al.* 2023). In addition, the WFC Project was also required to conduct the wheat–rice rotation, so these agricultural rotation systems were also set for simulation, and the details are shown in Appendix D.

2.5. Pearson correlation analysis

Pearson correlation analysis is a statistical method widely used to measure the correlation between two observations

Table 1 The critical parameters set in the CENTURY model for traditional farmland or well-facilitated farmland

	Parameters	Well-facilitated farmland		Definition
		No	Yes	
Site information	NLYER	1		Total layers in solum
Harvest	AGLREM	0.10	0.45	Fraction of aboveground live which will not be affected by harvest operations
Irrigation	FAWHC	Wheat=0.15 Rice=0.50	Wheat=0.25 Rice=0.95	Fraction of available water holding capacity below
Fertilization	FERT	Wheat=3.50 Rice=15.00		Amount of nitrogen to be added

by calculating the score (ranging from –1 to 1). This study applied the Pearson correlation analysis to show the interrelations between the SOCD and the other soil properties (pH, BD, and soil texture). The correlation analysis was conducted with R 4.2.1 (R Core Team 2022).

2.6. Performance evaluation

The soil sample dataset was randomly divided into the training set (60%) and the testing set (40%), which have different applications for RF and CENTURY models (Bista *et al.* 2016; Zeraatpisheh *et al.* 2021). For the RF model, the training set was used to calibrate the *mtry* and *ntree*, and the testing set was applied to independence verification; for the CENTURY model, the training set was used to adjust and calibrate the parameters (such as soil information, climate characteristics, agricultural system, and other relevant factors) to ensure the model accurately represented the farmland ecosystem of the study area, as well as the testing set was used to verify the model accuracy. Several statistical metrics were employed to evaluate the performance of the models. Normalized root mean square error (NRMSE) is a useful indicator with dimensionless, and the performance was generally acceptable with the NRMSE below 50% (Beusen *et al.* 2015; Priesack *et al.* 2016; Zhang *et al.* 2018). Besides, the coefficient of determination (R^2), the root mean square error (RMSE), and the mean absolute error (MAE) were also selected to evaluate the RF and CENTURY model. The equations are as follows:

$$R^2=1-\frac{\sum_i^n(\hat{y}_i-y_i)^2}{\sum_i^n(y_i-\bar{y})^2} \quad (3)$$

$$\text{NRMSE}=\frac{\sqrt{\frac{\sum_i^n(\hat{y}_i-y_i)^2}{n}}}{\bar{y}} \quad (4)$$

$$\text{RMSE}=\sqrt{\frac{\sum_i^n(\hat{y}_i-y_i)^2}{n}} \quad (5)$$

$$\text{MAE}=\frac{1}{n}\sum_i^n|(y_i-\hat{y}_i)| \quad (6)$$

where n represents the number of samples, y_i and $\hat{y}_i$ are the observations and predictions for sample i, respectively. $\bar{y}$ is the average of observations. These indicators were calculated in R 4.2.1 (R Core Team 2022).

3. Results and discussion

3.1. The descriptive statistics of soil properties

The descriptive statistics of SOCD, pH, BD, sand, silt, and clay in the study area are shown in Table 2. The SOCD ranged from 1.23 to 6.35 kg m^{-2} with a mean value of 3.68 kg m^{-2}. The mean value of soil pH was 6.18, with a skewness of 0.62, indicating that the soil was weakly acidic. The BD was between 0.39 and 1.54 g cm^{-3}, with an average value of 1.12 g cm^{-3}. In terms of soil texture, we found sand was the predominant component with a mean value of 63.36%, followed by clay (29.08%), suggesting that the coarse particles dominate the soil texture of the study area. The coefficient of variation (CV) of the silt was the highest, with a value of 42.81%, indicating that there were outliers in the silt data.

The SOCD exhibited a skewness of –0.04 and a kurtosis of –0.46 (close to zero), indicating an approximately normalized distribution, while the skewness of sand and silt were –2.27 and 1.18, representing that the data distribution of these two properties showed skew to the left and right, as well as influenced the external factors. The kurtosis of sand is much higher than the other five soil properties, suggesting numerous large particles in soils.

3.2. The correlation between the SOCD and soil properties

The correlation between the SOCD and soil properties is shown in Table 3. SOCD had a robust negative correlation with pH (–0.64), indicating that the soil pH might influence the carbon cycle process. Notably, SOCD showed a negative correlation with sand content (–0.35) but a positive correlation with clay content (0.54), indicating that higher clay content tends to enhance SOCD. Additionally, BD and silt content had slight negative influences on SOCD, with correlation coefficients of –0.12 and –0.21, respectively. According to the correlation analysis, soil pH, clay, and sand were most associated with the spatio-temporal variation of SOCD.

3.3. Digital mapping of soil properties

The RF model was applied to predict spatial patterns of key soil properties, including SOCD (sampling in 2023), pH, BD, sand, silt, and clay content. To assess the predictive accuracy of the RF model, the sample dataset was randomly divided into a training set and a testing set, and the NRMSE, R^2, RMSE, and MAE were selected as the evaluation indicators.

The model performance of soil properties using DSM In this study, the training set was used to calibrate the parameters of the RF model, while the testing set was used to validate the predicted results and assess the model

Table 2 The description of soil properties[1)]

Soil properties[2)]	Min.	Max.	Mean	SD	CV (%)	Skewness	Kurtosis
SOCD (kg m^{-2})	1.23	6.35	3.68	1.03	28.09	–0.04	–0.46
pH	3.98	8.47	6.18	0.88	14.21	0.62	0.01
BD (g cm^{-3})	0.39	1.54	1.12	0.18	16.09	–0.28	0.76
Sand (%)	17.92	76.56	63.36	5.49	8.66	–2.27	23.03
Silt (%)	2.00	20.00	7.30	3.13	42.81	1.18	2.30
Clay (%)	11.56	37.92	29.08	5.50	18.93	–1.60	2.29

[1)] SD, standard deviation; CV, coefficient of variation.
[2)] SOCD, soil organic carbon density; BD, bulk density.

performance. The accuracy of the RF model is summarized in Table 4. The values of the NRMSE were below 50%, and the R^2 ranged from 0.22 to 0.41, indicating that the model performance was within the acceptable range. The results represented that RF for predicting sand obtained the best performance with the lowest uncertainty (NRMSE=7.11%, R^2=0.37, RMSE=4.54, and MAE=3.54); in contrast, the accuracy of RF for silt spatial prediction produced the worst performance (NRMSE=47.46%, R^2=0.22, RMSE=3.63, and MAE=2.63), this lower accuracy for silt prediction might be attributed to the high data dispersion and presence of outliers in the silt dataset (CV of 42.81%). Additionally, the spectra and remote sensing indicators responding to the silt component might be less significant than other soil properties (Swain *et al.* 2021). For SOCD, pH, BD, and clay, the NRMSE was 26.50, 12.76, 15.64, and 21.10%, respectively. Overall, the RF could accurately predict the spatial distribution of soil critical parameters and provide the required soil information for SOCD dynamics simulation using the CENTURY model.

The spatial distribution of the SOCD and soil properties Fig. 3 illustrates the spatial distribution of SOCD, pH, BD, sand, silt, and clay (sampling in 2023). High SOCD values were predominantly concentrated in the western and southern regions of the study area, whereas the lower SOCD was observed in the central (around the water area) and eastern areas (Fig. 3-A). We noted that the distribution of clay was similar to the spatial pattern of SOCD (Fig. 3-F), while the distribution of sand content exhibited the inverse trend (Fig. 3-D). This observation aligns with the correlation analysis, which revealed a positive relationship between SOCD and clay content and a negative relationship between SOCD and sand content (Table 3). According to previous studies, it was commonly difficult to maintain organic carbon in sandy soil after the litter breakdown by microbes (Six *et al.* 1999; Gabarrón-Galeote *et al.* 2015; Yost and Hartemink 2019). However, the characteristic of clay was the adsorption capacity, which could protect more organic carbon from leaching by increasing the occlusion in micro-aggregates (Tisdall and Oades 1982; Baldock and Skjemstad 1999). Besides, clay soils retained higher soil moisture, indirectly improving SOC sequestration (Chen *et al.* 2019; Schapel *et al.* 2019). The spatial pattern of silt was different from the other soil properties, which randomly distributed high-value areas in the study area (Fig. 3-E), indicating that the percentage of silt had a slight influence on the SOCD.

Furthermore, the high-value area of the pH and BD was scattered in the eastern and central parts, corresponding to the lower-value areas of SOCD (Fig. 3-B and C). Soil acidification could reduce microbial activity and decrease the decomposition rate of humus, thereby influencing the SOC dynamics (McCauley *et al.* 2009; Sul *et al.* 2013). As an important physical parameter for SOCD calculation, BD was associated with soil aeration and moisture, and the previous research reported that suitable aeration and moisture contributed to crop yield and root growth, meaning that more organic matter might enter the soil and increase the SOCD (Erbach 1987; Czyż 2004; Chen *et al.* 2024). These findings underscored the significant influence of pH, BD, sand, silt, and clay content on the spatial distribution of SOCD. Therefore, the farmland construction initiatives should prioritize the impacts of these soil properties on SOCD and implement continuous monitoring to ensure soil health and sustainability following well-facilitated construction projects in the future.

Table 3 The correlation analysis between the soil organic carbon density (SOCD) and soil parameters[1)]

	SOCD	pH	BD	Sand	Silt	Clay
SOCD	–					
pH	–0.64**	–				
BD	–0.12	0.50**	–			
Sand	–0.35**	0.46**	0.32**	–		
Silt	–0.21**	0.38**	0.13**	–0.05	–	
Clay	0.54**	–0.73**	–0.38**	–0.57**	–0.59**	–

[1)] BD, bulk density.
** represents significance at the 0.01 level.

Table 4 The accuracy of soil critical properties mapping by Random Forest model using the testing dataset (sampling time: 2023)[1)]

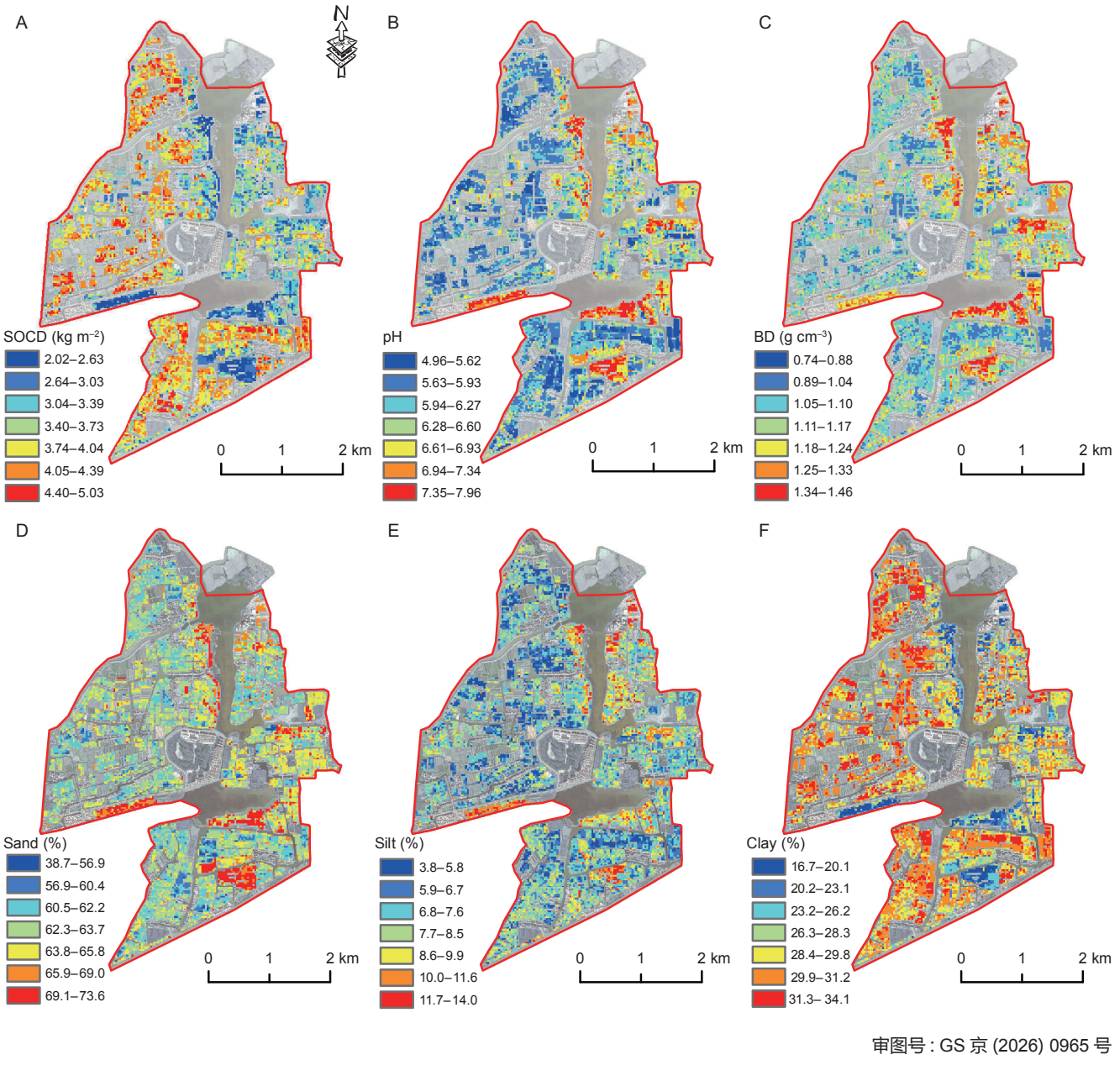
Soil properties[2)]	NRMSE (%)	R^2	RMSE	MAE
SOCD (kg m^{-2})	26.50	0.41	0.97	0.80
pH	12.76	0.36	0.80	0.62
BD (g cm^{-3})	15.64	0.30	0.18	0.14
Sand (%)	7.11	0.37	4.54	3.54
Silt (%)	47.46	0.22	3.63	2.63
Clay (%)	21.10	0.34	6.01	4.32

[1)] NRMSE, normalized root mean square error; RMSE, root mean square error; MAE, mean absolute error.
[2)] SOCD, soil organic carbon density; BD, bulk density.

3.4. The spatio-temporal simulation of SOCD by CENTURY

The model performance of the CENTURY To adapt the CENTURY model to the farmland ecosystem of this study, the training set was used to calibrate the default parameters, while the testing set was utilized to assess the CENTURY model performance. The results demonstrated that the CENTURY model performed slightly better than the Random Forest (RF) model in predicting SOCD (Table 5). The NRMSE was below 50% with R^2 of 0.30 and 0.34, indicating that the performance of the CENTURY model was considerable. Consequently, the CENTURY model captured the spatio-temporal variation of SOCD in the study area.

The history and future changes of SOCD The temporal change of SOCD was simulated using the CENTURY model, and the results are presented in Fig. 4. Before the implementation of the WFC Project, the SOCD exhibited a decreasing trend from 2010 to 2021; but, following the WFC Project (2022–2030), the trend reversed, showing an increase in SOCD (red line in Fig. 4). For comparison, a hypothesis scenario was simulated to illustrate SOCD trend without the WFC Project in the future decades (blue line in Fig. 4); the results showed that the SOCD would continuously decline from 2022 to 2030, even the value in 2030 was lower than those in the 1980s (3.21 kg m^{-2}) (Xu *et al.* 2006). The declining trend of SOCD might be associated with inadequate



审图号 : GS 京 (2026) 0965 号

Fig. 3 The spatial distribution of soil organic carbon density (SOCD) and other soil properties in 2023 using digital soil mapping technology. A, SOCD. B, pH. C, bulk density. D, sand. E, silt. F, clay. The background is the remote sensing image of the study area.

irrigation and not conducting straw incorporation, which decreased the carbon input and sequestration capacity. In addition, we also calculated the SOCD of the study area in the 2010s using soil sampling sites from project of the National Soil Series Survey and Compilation of Soil Series of China (2009–2019) (Liu *et al.* 2022), the average value was the 4.12 kg m^{-2}, which closely matched the 2010 value simulated by the CENTURY model but was significantly higher than the projected 2030 value under the hypothetical scenario. Therefore, the SOCD trend was related to optimizing irrigation and harvesting approaches, and the WFC Project was essential for farmland soil carbon sequestration.

The WFC required improved irrigation to increase soil moisture in farmland, which had profound implications for crop growth, soil erosion resistance, and carbon mineralization rate in the farmland ecosystem. The previous studies demonstrated that an appropriate irrigation approach could enhance crop yield, potentially increasing the litter input into the soil (Collins *et al.* 1992). Moreover, irrigation accelerated the weathering process and made the soil particle size smaller, which implied that the soil could adsorb more SOC (Presley *et al.* 2004). Neufeldt (2005) also reported that the high soil moisture reduced the mineralization rate, benefiting SOC storage.

In addition to irrigation, straw incorporation could substantially improve organic carbon storage (Xu *et al.* 2011; Cong *et al.* 2020). The WFC Project promotes straw incorporation as an alternative to traditional harvest practices (complete crop removal); this approach compensated for the loss of native SOC in the cropland and significantly

Table 5 The accuracy assessment of the CENTURY model[1)]

Data set	NRMSE (%)	R^2	RMSE	MAE
Training set (kg m^{-2})	24.78	0.30	0.90	0.74
Testing set (kg m^{-2})	25.03	0.34	0.92	0.73

[1)] NRMSE, normalized root mean square error; RMSE, root mean square error; MAE, mean absolute error.

increased the amount of litter entering the soil; for instance, Wu *et al.* (2019) found that straw-driven SOC inputs not only compensated for SOC losses due to mineralization but also enhanced overall carbon sequestration. Moreover, straw incorporation improved the growth and diversity of soil abundance of carbon-related microflora by optimizing the soil pH, significantly increasing the rate of decomposition of the litter into SOC (Sarkar *et al.* 2006; Lin *et al.* 2025).

In conclusion, the irrigation and harvest practices specified by the WFC Project could improve the soil function, increase or maintain the SOCD levels in the future, and indirectly promote the soil organic matter (SOM) contents and crop productivity. Conversely, if the well-facilitated farmland was not constructed and stayed in the situation of traditional farmland, SOCD would decline, potentially leading to a decrease in grain yield in the future.

The spatial distribution of SOCD in the history and future Fig. 5 illustrates the historical and future spatial distribution of SOCD simulated by the CENTURY model. The WFC Project in Jiashan was completed in 2022, so the SOCD in 2010, 2021, and 2030 represented the spatial distribution before, during, and after the implementation of the WFC Project. The spatial structure of SOCD for these three periods was similar (Fig. 5-A–C) and also corresponded to the spatial pattern in 2023 (Fig. 3-A), representing that the same environmental factors (pH, BD, and soil texture) likely governed the spatial patterns of SOCD within individual periods (2010, 2021, and 2030), while the long-term variation (2010–2030) of SOCD was also related to the SOC input (like straw incorporation increasing the SOC) besides the soil properties. Hence, it could be inferred that the WFC Project enhanced the SOCD across the entire farmland, but it did not specifically address low SOCD values in specific field plots. Nevertheless, the spatial distribution of SOCD trends and slopes after the WFC Project also demonstrated that SOCD would increase in the future (Appendix E). Notably, areas with lower SOCD in 2021 exhibited a faster rate of increase, and the difference in SOCD increase rates between low-value and high-value areas was statistically significant (P<2.2e^{-16}, t-test), highlighting the substantial carbon sequestration potential of these regions. Therefore, the WFC Project should pay more attention to specific fields with low SOCD, aiming to realize refined management of farmland soil and improve crop yield.

3.5. Limitations and perspectives

The CENTURY model could simulate the spatio-temporal variation of SOC by incorporating a wide range of parameters, including climate, soil, crop, and agricultural activities. However, obtaining all necessary parameters could be challenging, and the complexity of the farmland soil environment, influenced by both natural and anthropogenic factors, makes it difficult for process-based models to simulate carbon dynamics perfectly. Therefore, soil information, including pH, BD, and soil texture, was collected from the field investigation in this study. Climate data and fertilization practices were derived from the literature, while the agricultural system was based on expert knowledge. However, there were other parameters in the CENTURY model, and only using this information might decrease the accuracy of the simulation. Therefore, future studies should aim to gather the most reliable information to enhance simulation precision. Additionally, a notable limitation of the CENTURY model was the lack of a built-in function for uncertainty analysis. Developing methods to quantify and incorporate uncertainty into simulations using the CENTURY model was an important area for future research.

Secondly, the WFC was a national initiative with significant implications for farmland soil (Wang *et al.* 2020). While this study focused on SOC variation at a regional scale and considered only the soil thickness, harvest, and irrigation, other factors outlined in the WFC Project were not included. In addition, we also planned to explore the SOC dynamics of long-term scales under the future climate data (e.g., CMIP6), with the purpose of finding out the influence of the WFC Project on agricultural soil carbon cycle, soil health, and crop productivity. Therefore, the next step will involve exploring the historical trends and future changes of SOC at a national scale, incorporating additional factors.

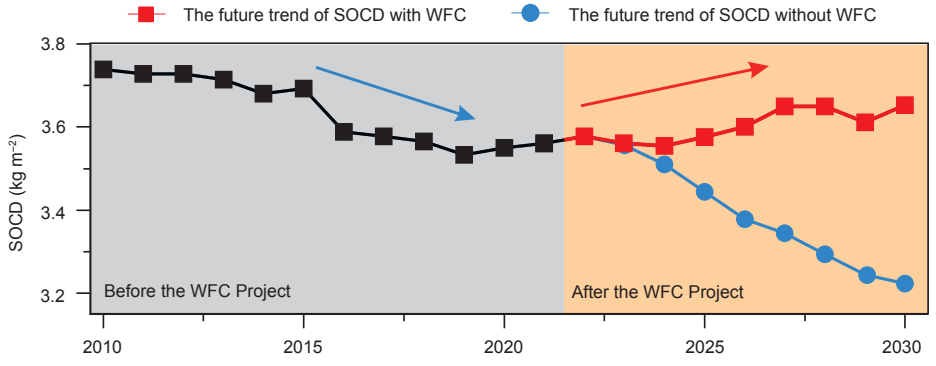
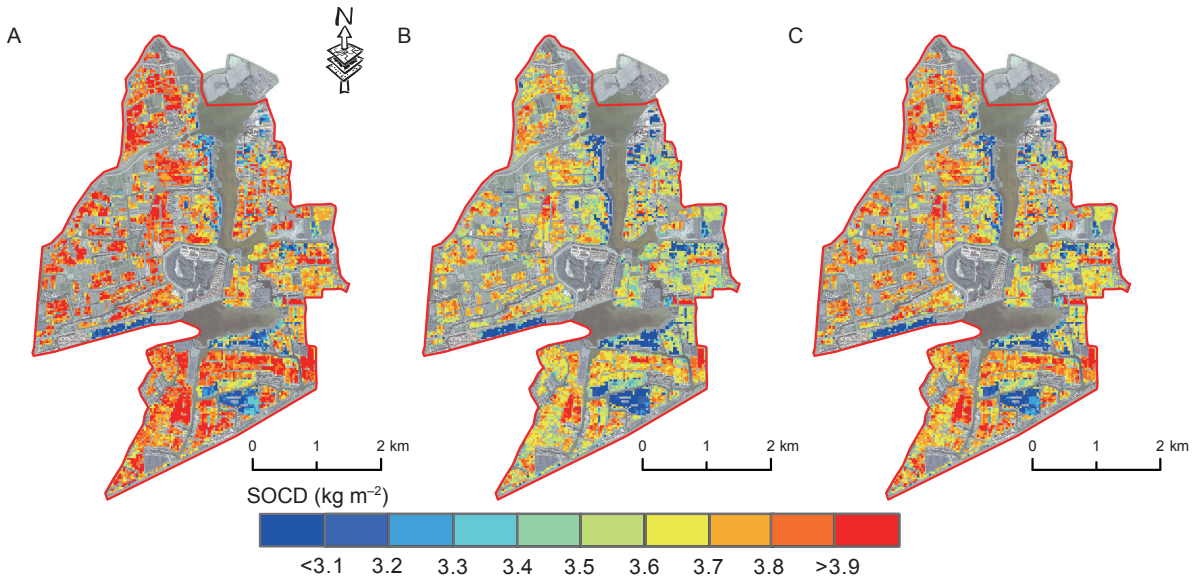


Fig. 4 The historical and future trends of soil organic carbon density (SOCD) changes. WFC, Well-facilitated Farmland Construction.



审图号：GS 京 (2026) 0965 号

Fig. 5 The soil organic carbon density (SOCD) changes before and after the Well-facilitated Farmland Construction. A, 2010. B, 2021. C, 2030.

Thirdly, SOC in farmland soil is closely linked to crop production, with food security being a key objective of the WFC Project. However, not only total SOC but also its fractions (particulate organic carbon and mineral-associated organic carbon) play critical roles in farmland ecosystems (Lavallee *et al.* 2020; Xiao *et al.* 2022; Dai *et al.* 2025). Moving from conceptual C pool-based models (e.g., RothC and Century) to measurable C pool-based models (e.g., MEMS) would enable a more robust simulation of SOC dynamics (Zhang *et al.* 2021). Furthermore, SOC is related to climate change, which affects carbon input to the soil. Therefore, the spatio-temporal dynamics of SOC and its relationship with crop growth should be further explored using process-based models under the different future climate scenarios.

4. Conclusion

In this study, we used the DSM and CENTURY to simulate the SOCD dynamics influenced by the WFC Project based on the field soil observations. The main conclusions are as follows: (1) Soil pH, sand, and clay were the primary factors influencing the SOCD; the high pH and sand component would decrease the SOCD, whereas the high clay component would protect more organic carbon in the soil. (2) The decreasing trend of SOCD from 2010 to 2021 was significantly halted, and SOCD was projected to increase in the future, as simulated by the CENTURY model; while the SOCD would have continued to decline from 2021 to 2030, if not for carrying out the WFC Project. Therefore, it can be concluded that the WFC Project is a practical approach to preventing SOC loss in farmland. (3) The spatial patterns of SOCD were similar during 2010–2030, indicating that soil with low SOCD could sequester more carbon in specified field plots by improving soil properties and agricultural activities. In conclusion, the requirements implemented by the WFC Project could improve the SOCD and SOM in the paddy soil, and these improvements contributed to better soil management, enhanced food security, and climate change mitigation.

Acknowledgements

This research is supported by the National Key Research and Development Program of China (2022YFB3903505 and 2022YFB3903503). We highly appreciate the great efforts from two anonymous reviewers for their constructive comments.

Declaration of competing interest

The authors declare that they have no conflict of interest.

Declaration of generative AI and AI-assisted technologies in the writing process

The authors declare that they did not use AI in the preparation and writing of this manuscript.

Appendices associated with this paper are available at https://doi.org/10.1016/j.jia.2025.11.006

References

Allison F E. 1973. *Soil Organic Matter and its Role in Crop Production*. Elsevier, New York.

Baldock J A, Skjemstad J O. 1999. Soil organic carbon/soil organic matter. In: Peverill K, Reuter D, Sparrow L, eds., *Soil Analysis-An Interpretation Manual*. CSIRO Publishing, Melbourne, Vic. Australia. pp. 159–170.

Bao S. 2000. *Soil Agrochemical Analysis*. China Agriculture Press, Beijing, China. (in Chinese)

Bauer A, Black A L. 1994. Quantification of the effect of soil organic matter content on soil productivity. *Soil Science Society of America Journal*, **58**, 185–193.

Behrens T, Schmidt K, Ramirez-Lopez L, Gallant J, Zhu A X, Scholten T. 2014. Hyper-scale digital soil mapping and soil formation analysis. *Geoderma*, **213**, 578–588.

Ben-Dor E, Patkin K, Banin A, Karnieli A. 2002. Mapping of several soil properties using DAIS-7915 hyperspectral scanner data — a case study over clayey soils in Israel. *International Journal of Remote Sensing*, **23**, 1043–1062.

Berardi D, Brzostek E, Blanc-Betes E, Davison B, DeLucia E H, Hartman M D, Kent J, Parton, W J, Saha D, Hudiburg T W. 2020. 21st-century biogeochemical modeling: Challenges for Century-based models and where do we go from here? *GCB Bioenergy*, **12**, 774–788.

Beusen A H W, Van Beek L P H, Bouwman A F, Mogollón J M, Middelburg J J. 2015. Coupling global models for hydrology and nutrient loading to simulate nitrogen and phosphorus retention in surface water-description of IMAGE-GNM and analysis of performance. *Geoscientific Model Development*, **8**, 4045–4067.

Bista P, Machado S, Ghimire R, Del Grosso S J, Reyes-Fox M. 2016. Simulating soil organic carbon in a wheat-fallow system using the daycent model. *Agronomy Journal*, **108**, 2554–2565.

Blanco-Canqui H, Shapiro C A, Wortmann C S, Drijber R A, Mamo M, Shaver T M, Ferguson R B. 2013. Soil organic carbon: The value to soil properties. *Journal of Soil and Water Conservation*, **68**, 129A–134A.

Breiman L. 2001. Random forests. *Machine Learning*, **45**, 5–32.

Cambule A H, Rossiter D G, Stoorvogel J J. 2013. A methodology for digital soil mapping in poorly-accessible areas. *Geoderma*, **192**, 341–353.

Chen S, Arrouays D, Angers D A, Chenu C, Barré P, Martin M P, Saby N P, Walter C. 2019. National estimation of soil organic carbon storage potential for arable soils: A data-driven approach coupled with carbon-landscape zones. *Science of the Total Environment*, **666**, 355–367.

Chen S, Arrouays D, Leatitia Mulder V, Poggio L, Minasny B, Roudier P, Libohova Z, Lagacherie P, Shi Z, Hannam J, Meersmans J, Richer-de-Forges A C, Walter C. 2022. Digital mapping of GlobalSoilMap soil properties at a broad scale: A review. *Geoderma*, **409**, 115567.

Chen S, Chen Z, Zhang X, Luo Z, Schillaci C, Arrouays D, Richer-de-Forges A C, Shi Z. 2024. European topsoil bulk density and organic carbon stock database (0–20cm) using machine-learning-based pedotransfer functions. *Earth System Science Data*, **16**, 2367–2383.

Chen S, Martin M P, Saby N P, Walter C, Angers D A, Arrouays D. 2018. Fine resolution map of top-and subsoil carbon sequestration potential in France. *Science of the Total Environment*, **630**, 389–400.

Chen S, Zhang G, Wang C. 2023. How does straw-incorporation rate reduce runoff and erosion on sloping cropland of black soil region? *Agriculture*, *Ecosystems & Environment*, **357**, 108676.

Chen Z, Shuai Q, Shi Z, Arrouays D, Richer-de-Forges A C, Chen S. 2023. National-scale mapping of soil organic carbon stock in France: New insights and lessons learned by direct and indirect approaches. *Soil & Environmental Health*, **1**, 100049.

Chen Z M, Wang H Y, Liu X W, Zhao X L, Lu D J, Zhou J M, Li C Z. 2017. Changes in soil microbial community and organic carbon fractions under short-term straw return in a rice–wheat cropping system. *Soil and Tillage Research*, **165**, 121–127.

Collins H P, Rasmussen, P E, Douglas C L. 1992. Crop rotation and residue management effects on soil carbon and microbial dynamics. *Soil Science Society of America Journal*, **56**, 783–788.

Cong P, Wang J, Li Y, Liu N, Dong J, Pang H, Zhang L, Gao Z. 2020. Changes in soil organic carbon and microbial community under varying straw incorporation strategies. *Soil and Tillage Research*, **204**, 104735.

Czyż E A. 2004. Effects of traffic on soil aeration, bulk density and growth of spring barley. *Soil and Tillage Research*, **79**, 153–166.

Dai L, Wang Z, Zhuo Z, Ma Y, Shi Z, Chen S. 2025. Prediction of soil organic carbon fractions in tropical cropland using a regional visible and near-infrared spectral library and machine learning. *Soil and Tillage Research*, **245**, 106297.

Dai L, Xue J, Lu R, Wang Z, Chen Z, Yu Q, Shi Z, Chen S. 2024. *In-situ* prediction of soil organic carbon contents in wheat–rice rotation fields via visible near-infrared spectroscopy. *Soil & Environmental Health*, **2**, 100113.

Dharumarajan S, Hegde R. 2020. Digital mapping of soil texture classes using Random Forest classification algorithm. *Soil Use and Management*, **38**, 135–149.

Dimassi B, Guenet B, Saby N P A, Munoz F, Bardy M, Millet F, Martin M P. 2018. The impacts of CENTURY model initialization scenarios on soil organic carbon dynamics simulation in French long-term experiments. *Geoderma*, **311**, 25–36.

Dong B, Liu H, Wang Y, Qiao Y, Zhang M, Yang H, Jin L, Liu M. 2018. Physio-ecological regulating mechanisms for highly efficient water use of crops. *Chinese Journal of Eco-Agriculture*, **26**, 1465–1475. (in Chinese)

Erbach D C. 1987. Measurement of soil bulk density and moisture. *Transactions of the ASAE*, **30**, 922–931.

Eswaran H, Van Den Berg E, Reich P. 1993. Organic carbon in soils of the world. *Soil Science Society of America Journal*, **57**, 192–194.

Franzluebbers A J. 2002. Soil organic matter stratification ratio as an indicator of soil quality. *Soil and Tillage Research*, **66**, 95–106.

Gabarrón-Galeote M A, Trigalet S, van Wesemael B. 2015. Effect of land abandonment on soil organic carbon fractions along a Mediterranean precipitation gradient. *Geoderma*, **249–250**, 69–78.

Gao B C, Goetz A F, Wiscombe W J. 1993. Cirrus cloud detection from airborne imaging spectrometer data using the 1.38 μm water vapor band. *Geophysical Research Letters*, **20**, 301–304.

Gholizadeh A, Žižala D, Saberioon M, Borůvka L. 2018. Soil organic carbon and texture retrieving and mapping using proximal, airborne and Sentinel-2 spectral imaging. *Remote Sensing of Environment*, **218**, 89–103.

Goidts E, Van Wesemael B, Crucifix M. 2009. Magnitude and sources of uncertainties in soil organic carbon (SOC) stock assessments at various scales. *European Journal of Soil Science*, **60**, 723–739.

Grimm R, Behrens T, Märker M, Elsenbeer H. 2008. Soil organic carbon concentrations and stocks on Barro Colorado Island-Digital soil mapping using Random Forests analysis. *Geoderma*, **146**, 102–113.

Hengl T, Heuvelink G B, Kempen B, Leenaars J G, Walsh M G, Shepherd K D, Sila A, MacMillan R A, Mendes de Jesus J, Tamene L, Tondoh J E. 2015. Mapping soil properties of Africa at 250m resolution: Random Forests significantly improve current predictions. *PLoS ONE*, **10**, e0125814.

Heung B, Bulmer C E, Schmidt M G. 2014. Predictive soil parent material mapping at a regional-scale: A Random Forest approach. *Geoderma*, **214–215**, 141–154.

Inman D J, Freeland R S, Ammons J T, Yoder R E. 2002. Soil investigations using electromagnetic induction and Ground — Penetrating Radar in southwest Tennessee. *Soil Science Society of America Journal*, **66**, 206–211.

Jin X, Du J, Liu H, Wang Z, Song K. 2016. Remote estimation of soil organic matter content in the Sanjiang Plain, Northest China: The optimal band algorithm versus the GRA-ANN model. *Agricultural and Forest Meteorology*, **218**, 250–260.

Kelly R H, Parton W J, Crocker G J, Graced P R, Klír J, Körschens M, Poulton P R, Richter D D. 1997. Simulating trends in soil organic carbon in long-term experiments using the century model. *Geoderma*, **81**, 75–90.

Kumar N, Velmurugan, Hamm N A S, Dadhwal V K. 2018. Geospatial mapping of soil organic carbon using regression kriging and remote sensing. *Journal of the Indian Society of Remote Sensing*, **46**, 705–716.

Lagacherie P, McBratney A B. 2006. Spatial soil information systems and spatial soil inference systems: perspectives for digital soil mapping. *Developments in Soil Science*, **31**, 3–22.

Lal R. 2013. Intensive agriculture and the soil carbon pool. *Journal of Crop Improvement*, **27**, 735–751.

Lavallee J M, Soong J L, Cotrufo M F. 2020. Conceptualizing soil organic matter into particulate and mineral-associated forms to address global change in the 21st century. *Global Change Biology*, **26**, 261–273.

Li M, Zhang X, Pang G, Han F. 2013. The estimation of soil organic carbon distribution and storage in a small catchment area of the Loess Plateau. *Catena*, **101**, 11–16.

Liang F, Li B, Vog, R D, Mulder J, Song H, Chen J, Guo J. 2023. Straw return exacerbates soil acidification in major Chinese croplands. *Resources*, *Conservation and Recycling*, **198**, 107176.

Liaw A, Wiener M. 2002. Classification and regression by random forests. *R News,* **2–3**, 18–22

Lin H, Zheng J, Zhou M, Xu P, Lan T, Kuang F, Li Z, Yao Z, Zhu B.

2025. Crop straw incorporation increases the soil carbon stock by improving the soil aggregate structure without stimulating soil heterotrophic respiration. *Journal of Integrative Agriculture,* **24**, 1542–1561.
Liu F, Wu H, Zhao Y, Li D, Yang J L, Song X, Shi Z, Zhu A X, Zhang G L. 2022. Mapping high resolution National Soil Information Grids of China. *Science Bulletin*, **67**, 328–340.
Liu S, An N, Yang J, Dong S, Wang C, Yin Y. 2015. Prediction of soil organic matter variability associated with different land use types in mountainous landscape in southwestern Yunnan province, China. *Catena*, **133**, 137–144.
Long J, Liu Y, Xing S, Zhang L, Qu M, Qiu L, Huang Q, Zhou B, Shen J. 2020. Optimal interpolation methods for farmland soil organic matter in various landforms of a complex topography. *Ecological Indicators*, **110**, 105926.
Malone B P, Minasny B, Odgers N P, McBratney A B. 2014. Using model averaging to combine soil property rasters from legacy soil maps and from point data. *Geoderma*, **232–234**, 34–44.
Mao Z. 2002. Water saving irrigation for rice and its effect on environment. *Engineering Science*, **4**, 8–16. (in Chinese)
McBratney A B, Mendonça Santos M L, Minasny B. 2003. On digital soil mapping. *Geoderma*, **117**, 3–52.
McCauley A, Jones C, Jacobsen J. 2009. Soil pH and organic matter. *Nutrient Management Module*, **8**, 1–12.
Minasny B, McBratney A B. 2016. Digital soil mapping: A brief history and some lessons. *Geoderma*, **264**, 301–311.
NDRC (National Development and Reform Commission). 2021. National Well-facilitated Farmland Construction Plan (2021–2030). [2021-11-2]. https://www.ndrc.gov.cn/fggz/fzzlgh/gjjzxgh/202111/t20211102_1302810.html
Neufeldt H. 2005. Carbon stocks and sequestration potentials of agricultural soils in the federal state of Baden-Württemberg, SW Germany. *Journal of Plant Nutrition and Soil Science*, **168**, 202–211.
Ogle S M, Breidt F J, Easter M, Williams S, Killian K, Paustian K. 2010. Scale and uncertainty in modeled soil organic carbon stock changes for US croplands using a process-based model. *Global Change Biology*, **16**, 810–822.
Ouyang W, Shan Y, Hao F, Lin C. 2014. Differences in soil organic carbon dynamics in paddy fields and drylands in northeast China using the CENTURY model. *Agriculture*, *Ecosystems & Environment*, **194**, 38–47.
Parton W J, Stewart J W, Cole C V. 1988. Dynamics of C, N, P and S in grassland soils: A model. *Biogeochemistry*, **5**, 109–131.
Presley D R, Ransom M D, Kluitenberg G J, Finnell P R. 2004. Effects of thirty years of irrigation on the genesis and morphology of two semiarid soils in Kansas. *Soil Science Society of America Journal*, **68**, 1916–1926.
Priesack E, Gayler S, Hartmann H P. 2006. The impact of crop growth sub-model choice on simulated water and nitrogen balances. *Nutrient Cycling in Agroecosystems*, **75**, 1–13.
R Core Team. 2022. R: A language and environment for statistical computing. R foundation for statistical computing, Lanzhou, China.
Reijneveld A, van Wensem J, Oenema O. 2009. Soil organic carbon contents of agricultural land in the Netherlands between 1984 and 2004. *Geoderma*, **152**, 231–238.
Sanderman J, Hengl T, Fiske G J. 2017. Soil carbon debt of 12,000 years of human land use. *Proceedings of the National Academy of Sciences of the United States of America*, **114**, 9575–9580.
Sarkar D, Tarafdar J C, Kundu M C. 2006. Effect of changes of soil pH on microbial activity and availability of phosphorus and sulfur. *Environment and Ecology*, **24**, 200–202.
Schapel A, Marschner P, Churchman J. 2019. Influence of clay clod size and number for organic carbon distribution in sandy soil with clay addition. *Geoderma*, **335**, 123–132.
Seitz S, Goebes P, Puerta V L, Pereira E I P, Wittwer R, Six J, van der Heijden M G A, Scholten T. 2018. Conservation tillage and organic farming reduce soil erosion. *Agronomy for Sustainable Development*, **39**, 4.
Six J, Elliott E T, Paustian K. 1999. Aggregate and soil organic matter dynamics under conventional and no-tillage systems. *Soil Science Society of America Journal*, **63**, 1350–1358.
Smith P. 2005. An overview of the permanence of soil organic carbon stocks: Influence of direct human-induced, indirect and natural effects. *European Journal of Soil Science*, **56**, 673–680.
Somaratne S, Seneviratne G, Coomaraswamy U. 2005. Prediction of soil organic carbon across different land-use patterns. *Soil Science Society of America Journal*, **69**, 1580–1589.
Stockmann U, Padarian J, McBratney A, Minasny B, de Brogniez D, Montanarella L, Hong S Y, Rawlins B G, Field D J. 2015. Global soil organic carbon assessment. *Global Food Security*, **6**, 9–16.
Sul W J, Asuming-Brempong S, Wang Q, Tourlousse D M, Penton C R, Deng Y, Rodrigues J L M, Adiku S G K, Jones J W, Zhou J, Cole J R, Tiedje J M. 2013. Tropical agricultural land management influences on soil microbial communities through its effect on soil organic carbon. *Soil Biology and Biochemistry*, **65**, 33–38.
Sun B, Wang Y, Li Z, Gao W, Wu J, Li C, Song Z, Gao Z. 2019. Estimating Soil Organic Carbon Density in the otindag sandy land, Inner Mongolia, China, for modelling spatiotemporal variations and evaluating the influences of human activities. *Catena*, **179**, 85–97.
Swain S R, Chakraborty P, Panigrahi N, Vasava H B, Reddy N N, Roy S, Majeed I, Das, B S. 2021. Estimation of soil texture using Sentinel-2 multi-spectral imaging data: An ensemble modeling approach. *Soil and Tillage Research*, **213**, 105134.
Tisdall J M, Oades J M. 1982. Organic matter and water-stable aggregates in soils. *Journal of Soil Science*, **33**, 141–163.
Tornquist C G, Mielniczuk J, Cerri C E P. 2009. Modeling soil organic carbon dynamics in Oxisols of Ibirubá (Brazil) with the Century Model. *Soil and Tillage Research*, **105**, 33–43.
Vaudour E, Gomez C, Fouad Y, Lagacherie P. 2019. Sentinel-2 image capacities to predict common topsoil properties of temperate and Mediterranean agroecosystems. *Remote Sensing of Environment*, **223**, 21–33.
Wang N, Chen S, Huang J, Frappart F, Taghizadeh R, Zhang X, Wigneron J P, Xue J, Xiao Y, Peng J, Shi Z. 2024. Global soil salinity estimation at 10m using multi-source remote sensing. *Journal of Remote Sensing*, **4**, 0130.
Wang X, Li Y, Lian J, Luo Y, Niu Y, Gong X. 2019. Progress in application of the CENTURY model for prediction of soil carbon levels in different ecosystems. *Acta Prataculturae Sinica*, **28**, 179-189. (in Chinese)
Wang X, Shi W, Sun X, Wang M. 2020. Comprehensive benefits evaluation and its spatial simulation for well-facilitated farmland projects in the Huang-Huai-Hai Region of China. *Land Degradation & Development*, **31**, 1837–1850.
Wang Y, Wu P, Mei F, Ling Y, Qiao Y, Liu C, Leghari S J, Guan X, Wang T. 2021. Does continuous straw returning keep China farmland soil organic carbon continued increase? A meta-analysis. *Journal of Environmental Management*, **288**, 112391.
Wu H, Guo Z, Peng C. 2003. Land use induced changes of organic carbon storage in soils of China. *Global Change Biology*, **9**, 305–315.
Wu L, Zhang W, Wei W, He Z, Kuzyakov Y, Bol R, Hu R. 2019. Soil organic matter priming and carbon balance after straw addition is regulated by long-term fertilization. *Soil Biology and Biochemistry*, **135**, 383–391.
Xiao Y, Xue J, Zhang X, Wang N, Hong Y, Jiang Y, Zhou Y, Teng H, Hu B, Lugato E, Richer-de-Forges A C. 2022. Improving pedotransfer functions for predicting soil mineral associated organic carbon by ensemble machine learning. *Geoderma*, **428**, 116208.
Xu M, Lou Y, Sun X, Wang W, Baniyamuddin M, Zhao K. 2011. Soil organic carbon active fractions as early indicators for total carbon change under straw incorporation. *Biology and Fertility of Soils*, **47**, 745–752.
Xu Q, Rui W, He H, Wu F, Luo H, Bian X, Zhang W. 2006. Characteristics and regional differences of soil organic carbon density in farmland under different land use patterns in China. *Scientia Agricultura Sinica*, **39**, 2505–2510. (in Chinese)
Xue J, Zhang X, Chen S, Hu B, Wang N, Shi Z. 2024. Quantifying the agreement and accuracy characteristics of four satellite-based LULC products for cropland classification in China. *Journal of Integrative Agriculture*, **23**, 283–297.
Yang J, Liu, K, Wang Z, Du Y, Zhang J. 2007. Water-saving and high-yielding irrigation for lowland rice by controlling limiting values of soil water potential. *Journal of Integrative Plant Biology*, **49**, 1445–1454.
Yang C, Wang X, Li J, Zhang G, Shu H, Hu W, Han H, Liu R, Guo Z. 2024. Straw return increases crop production by improving soil organic carbon sequestration and soil aggregation in a long-term wheat-cotton cropping system. *Journal of Integrative Agriculture*,

23, 669–679.
Yost J L, Hartemink A E. 2019. Soil organic carbon in sandy soils: A review. *Advances in Agronomy*, **158**, 217–310.
Zeraatpisheh M, Ayoubi S, Mirbagheri Z, Mosaddeghi M R, Xu M. 2021. Spatial prediction of soil aggregate stability and soil organic carbon in aggregate fractions using machine learning algorithms and environmental variables. *Geoderma Regional*, **27**, e00440.
Zhang H, Goll D S, Wang Y P, Ciais P, Wieder W R, Abramoff R, Huang Y, Guenet B, Prescher A K, Viscarra Rossel R A, Barre P, Chenu C, Zhou G, Tang X. 2020. Microbial dynamics and soil physicochemical properties explain large-scale variations in soil organic carbon. *Global Change Biology*, **26**, 2668–2685.
Zhang J, Balkovič J, Azevedo L B, Skalský R, Bouwman A F, Xu G, Wang J, Xu M, Yu C. 2018. Analyzing and modelling the effect of long-term fertilizer management on crop yield and soil organic carbon in China. *Science of the Total Environment*, **627**, 361–372.
Zhang L, Heuvelink G B M, Mulder V L, Chen S, Deng X, Yang L. 2024. Using process-oriented model output to enhance machine learning-based soil organic carbon prediction in space and time. *Science of the Total Environment*, **922**, 170778.
Zhang Y, Lavallee J M, Robertson A D, Even R, Ogle S M, Paustian K, Cotrufo M F, 2021. Simulating measurable ecosystem carbon and nitrogen dynamics with the mechanistically defined MEMS 2.0 model. *Biogeosciences*, **18**, 3147–3171.
Zhao R, Zhang W, Duan Z, Chen S, Shi Z. 2023. An improved estimate of soil carbon pool and carbon fluxes in the Qinghai-Tibetan grasslands using data assimilation with an ecosystem biogeochemical model. *Geoderma*, **430**, 116283.
Zhou F, Xue J, Wang Z, Jin W, Shi Z, Yu Q, Zhou L, Chen S. 2025. Integrating historical crop rotation changes into soil organic matter mapping in the cropland of southeastern China. *Earth's Future*, **13**, e2025EF006117.

Executive Editor-in-Chief Keke Yi
Managing Editor Lujuan Sun